Available online at www.sciencedirect.com
SCIENCE DIRECT®
Journal of Sound and Vibration 273 (2004) 33–49
JOURNAL OF SOUND AND VIBRATION
www.elsevier.com/locate/jsvi

Acoustic radiation from a plate into a porous medium

D. Tomlinson[a], R.J.M. Craik[a,*], R. Wilson[b]

[a] School of the Built Environment, Heriot-Watt University, Riccarton, Edinburgh EH14 4AS, UK
[b] School of the Built Environment, University of Nottingham, University Park, Nottingham NG7 2RD, UK

Received 14 December 2000; accepted 15 April 2003

Abstract

A theoretical model is developed for acoustic radiation from a plate into a porous medium. The medium is modelled as an equivalent fluid with complex density and complex wavespeed. It is found that radiation from a finite plate is dominated by area radiation at all frequencies, unlike the case for radiation into air where it is only area dependent above the critical frequency. Although particle motion is similar to that for radiation into air, the circulatory motion below the critical frequency still results in energy loss from the plate due to dissipation within the medium.

As radiation is area dependent at all frequencies, a simpler model based on radiation from an infinite plate is also developed. This gives the same answer as radiation from a finite plate to leading order. Plate losses measured for radiation into a finite thickness layer of porous material show good agreement with predicted results.

1. Introduction

Double walls represent an important class of structure widely used in vehicle design and building construction to provide good sound insulation with minimal mass. The air cavity created between the leaves of a double wall plays an important role, isolating the two structural elements from each other, hence reducing the vibration amplitude on the receiving side of the structure. An absorbent material may be placed in the cavity to damp the cavity modes and hence increase sound insulation.

The presence of absorbent materials in close proximity to (but not necessarily touching) structural elements has been observed to result in increased damping of the structure. A formulation of this problem for a finite plate radiating into a semi infinite half-space occupied by a

*Corresponding author. Tel.: +44-0131-449-5111; fax: +44-0131-451-3161.
E-mail address: r.j.m.craik@hw.ac.uk (R.J.M. Craik).

0022-460X/$ - see front matter
doi:10.1016/j.jsv.2003.04.003

porous material has been studied by Cummings et al. [1]. They studied the power radiated from a single plate mode into the porous medium, modelled using an equivalent fluid representation. Implicit in this approach therefore is that the vibrational field on the plate excites only the fluid contained within the porous medium and not the skeleton of the medium itself. The skeleton is in effect assumed to be rigid. The problem was tackled numerically as no analytical solution could be found. The results showed that for low order modes there is increased radiation into the porous material as compared with air, which may result in significant damping of the plate.

This paper describes an alternative analytic approach to solving the problem of radiation from a finite plate into porous media. It uses techniques adopted by Leppington et al. [2], who used asymptotic techniques to revisit the problem, previously treated by Maidanik [3], Wallace [4] and others, of radiation from a plate into air. When applied to the air problem, this approach provided additional insight to the radiation mechanisms.

In this paper the approach is used to examine radiation into a porous material that is represented as an equivalent fluid. The resulting analytical solution allows radiation from the plate to be predicted at high frequency where there are many modes and provides an insight into the physics involved. It is found that, for realistic porous materials, radiation is proportional to the plate area at all frequencies and that edge dependent effects are of secondary importance (in contrast to radiation into air where edge effects are dominant below the critical frequency, f_c). Therefore radiation can be found from consideration of an infinite plate that does not include edge effects. A simpler theory derived from consideration of an infinite plate is also presented and it is shown that identical results are obtained. These form the key findings of this paper.

The theoretical results are compared with measurements made on plates radiating into fibrous porous materials. There are no straightforward experiments to directly measure radiation into a porous layer and so indirect methods must be used. Radiation into a porous layer was determined from measurements of damping of a plate placed next to a porous layer. The measured results agree well with predictions based on the proposed model.

2. Radiation from a finite plate

2.1. Definition of the problem

A thin elastic plate occupies the region $0<x<a$, $0<y<b$, $z=0$ and is bounded by some porous medium represented by an equivalent fluid (with complex wave number k_a and complex density ρ_a) in the region $-\infty<x<\infty$, $-\infty<y<\infty$, $0<z<\infty$. The rest of the plane $z=0$ contains a rigid baffle. If the plate is simply supported and is excited by a sound field from the region $-\infty<x<\infty$, $-\infty<y<\infty$, $-\infty<z<0$ it will undergo vibrations with transverse velocity

$$U(x',y',t) = U_0 \sin k_x x' \sin k_y y' e^{i\omega t}, \tag{1}$$

where U_0 is the velocity amplitude. The plate wave numbers are given by $k_x = m\pi/a$ and $k_y = n\pi/b$ where (m and n are integers) and ω is the angular frequency. The co-ordinates (x', y') denote the position on the plate.

Following the method employed by Cummings et al. [1], the plate can be considered as an array of acoustic monopoles with volume velocity amplitudes Q_0. If a monopole is positioned at

$P'(x', y', 0)$ then its effect on the pressure at a general point $P(x, y, z)$ in the porous medium is

$$p'(r', t) = \frac{\mathrm{i}\omega\rho_a Q_0}{2\pi r'} \mathrm{e}^{-\mathrm{i}k_a r'}, \tag{2}$$

where $r'^2 = (x - x')^2 + (y - y')^2 + z^2$ is the square of the separation distance of P' and P.

The volume velocity of a monopole is given by the product of velocity and area thus,

$$Q_0 = U(x', y', t)\delta x'\delta y'. \tag{3}$$

Substituting the velocity from Eq. (1) into Eq. (3) and then using this in expression (2) for the pressure at $P(x, y, z)$ gives

$$p'(r', t) = \frac{\mathrm{i}\omega\rho_a U_0}{2\pi r'} \mathrm{e}^{\mathrm{i}\omega t} \sin k_x x' \sin k_y y' \mathrm{e}^{-\mathrm{i}k_a r'} \delta x'\delta y'. \tag{4}$$

The total pressure at $P(x, y, z)$ is given by the sum of the pressures from each point on the plate. This can be done by integrating (4) over the plate area to give

$$p(x, y, z, t) = \frac{\mathrm{i}\omega\rho_a U_0}{2\pi} \mathrm{e}^{\mathrm{i}\omega t} \int_0^b \int_0^a \sin k_x x' \sin k_y y' \frac{\mathrm{e}^{-\mathrm{i}k_a r'}}{r'} \mathrm{d}x' \, \mathrm{d}y'. \tag{5}$$

The total power, W, radiated from the plate is given by

$$W = \int_0^b \int_0^a \bar{I}(x, y) \, \mathrm{d}x \, \mathrm{d}y \quad \text{on } z = 0, \tag{6}$$

where

$$I(x, y, t) = \mathrm{Re}\{p(x, y, 0, t\}\mathrm{Re}\{U(x, y, 0, t)\}, \tag{7}$$

is the acoustic intensity normal to the plate. The bar denotes that a time-averaged quantity is required.

It should be noted that the power radiated cannot be determined from integration of the far field intensity, as can be done for air [4], since the medium is non-conservative and so power is dissipated within it.

This time-averaged intensity is given by

$$\bar{I}(x, y) = \frac{\omega}{2\pi} \int_0^{2\pi/\omega} I(x, y, t) \, \mathrm{d}t = \frac{1}{2} \mathrm{Re}\{p(x, y, 0, t) U^*(x, y, t)\}, \tag{8}$$

where the right-hand side of this is a consequence of the harmonic form of the time dependence. The superscript * denotes a complex conjugate.

Expression (5) on $z = 0$ now becomes

$$p(x, y, 0, t) = \frac{\mathrm{i}\omega\rho_a U_0}{2\pi} \mathrm{e}^{\mathrm{i}\omega t} \int_0^b \int_0^a \sin k_x x' \sin k_y y' \frac{\mathrm{e}^{-\mathrm{i}k_a r}}{r} \mathrm{d}x' \, \mathrm{d}y', \tag{9}$$

where $r^2 = (x - x')^2 + (y - y')^2$.

The velocity is also known from Eq. (1) giving

$$U(x, y, t) = U_0 \sin k_x x \sin k_y y \mathrm{e}^{\mathrm{i}\omega t}. \tag{10}$$

The wave number k_a is complex so it is useful to write it in the form $k_a = k(1 - \mathrm{i}\kappa)$. The real part of k_a is a measure of the phase velocity c_a of the wave and the imaginary part is related to the

sound attenuation with distance. The complex density can also be expressed in this form i.e., $\rho_a = \rho(1 - \mathrm{i}\tau)$. Note that this is the same as Cummings et al. [1] who expressed it as $\rho_a = |\rho'|\mathrm{e}^{\mathrm{i}\phi}$, where $|\rho'| = \rho(1+\tau^2)^{1/2}$ and $\phi = \tan^{-1}(-\tau)$.

Substituting these complex forms for k_a and ρ_a in Eqs. (9) and (10) gives the intensity defined by (8) as

$$\bar{I} = \frac{\omega\rho U_0^2}{4\pi}\left\{\int_0^b\int_0^a \sin k_x x \sin k_y y \sin k_x x' \sin k_y y' \frac{\sin kr}{r}\mathrm{e}^{-\kappa kr}\,\mathrm{d}x'\,\mathrm{d}y' + \tau\int_0^b\int_0^a \sin k_x x \sin k_y y \sin k_x x' \sin k_y y' \frac{\cos kr}{r}\mathrm{e}^{-\kappa kr}\,\mathrm{d}x'\,\mathrm{d}y'\right\} \tag{11}$$

and the power is then found by integrating this over the plate area as in Eq. (6). The term $\mathrm{e}^{-\kappa kr}$ accounts for the aforementioned dissipation in the medium.

It is useful to normalize this power with the power associated with a piston radiating into air. This gives a radiation efficiency, σ, thus

$$\sigma = \frac{W}{\rho_0 c_0 ab\langle U^2\rangle}, \tag{12}$$

where $\langle U^2\rangle$ is the mean square velocity averaged with respect to time and space (which in this case is equal to $\frac{1}{8}U_0^2$), ρ_0 is the mean density of air and c_0 is the wavespeed in air. Therefore, the expression for the radiation efficiency of the plate is

$$\sigma = \frac{2\omega\rho}{\rho_0 c_0 ab\pi}\left\{\int_0^b\int_0^a\int_0^b\int_0^a \sin k_x x \sin k_y y \sin k_x x' \sin k_y y' \frac{\sin kr}{r}\mathrm{e}^{-\kappa kr}\,\mathrm{d}x\,\mathrm{d}y\,\mathrm{d}x'\,\mathrm{d}y' + \tau\int_0^b\int_0^a\int_0^b\int_0^a \sin k_x x \sin k_y y \sin k_x x' \sin k_y y' \frac{\cos kr}{r}\mathrm{e}^{-\kappa kr}\,\mathrm{d}x\,\mathrm{d}y\,\mathrm{d}x'\,\mathrm{d}y'\right\}. \tag{13}$$

2.2. Comparison with sound radiation into air

A similar problem for sound radiation into a real fluid (air) was considered by Leppington et al. [2]. The equivalent expression for the radiation efficiency in this case is

$$\sigma_0 = \frac{2k_0}{\pi ab}\int_0^b\int_0^a\int_0^b\int_0^a \sin k_x x \sin k_y y \sin k_x x' \sin k_y y' \frac{\sin k_0 r}{r}\,\mathrm{d}x\,\mathrm{d}y\,\mathrm{d}x'\,\mathrm{d}y', \tag{14}$$

where $k_0 = \omega/c_0$ is the acoustic wavenumber of air. Here the omission of the exponentially decreasing term implies that the air is a conservative medium (assuming that no consideration is given to damping in the air i.e., k_0 is real). The method employed by Leppington et al. [2] to reduce the integral in Eq. (14) to an integral in a single variable is outlined below.

By letting J_0 be the integral in Eq. (14), σ_0 becomes

$$\sigma_0 = \frac{2k_0}{\pi ab}J_0. \tag{15}$$

If the transformations $x' = x + u$ and $y' = y + v$ are applied to J_0 such that $r^2 = u^2 + v^2$ and $\mathrm{d}x'\,\mathrm{d}y' = \mathrm{d}u\,\mathrm{d}v$ then the x and y integrals are independent of u and v and are easily performed

giving the following result

$$J_0 = \int_0^b \int_0^a \left\{ (a-u)\cos\alpha' k_0 u + \frac{1}{\alpha' k_0}\sin\alpha' k_0 u \right\} \times \left\{ (b-v)\cos\beta' k_0 v + \frac{1}{\beta' k_0}\sin\beta' k_0 v \right\} \frac{\sin k_0 r}{r}\,\mathrm{d}u\,\mathrm{d}v, \tag{16}$$

where $\alpha' = k_x/k_0$ and $\beta' = k_y/k_0$ are dimensionless wavenumbers, introduced for convenience.

By inspection the terms in the curly brackets can be rewritten as

$$a\cos\alpha' k_0 u - \frac{\alpha'}{k_0}\frac{\partial}{\partial\alpha'}\left(\frac{\sin\alpha' k_0 u}{\alpha'}\right) \quad \text{and} \quad b\cos\beta' k_0 v - \frac{\beta'}{k_0}\frac{\partial}{\partial\beta'}\left(\frac{\sin\beta' k_0 v}{\beta'}\right), \tag{17}$$

so J_0 can be expressed as

$$J_0 = abJ_1 + \frac{\alpha'\beta'}{k_0^2}\frac{\partial^2}{\partial\alpha'\ \partial\beta'}\left\{\frac{J_2}{\alpha'\beta'}\right\} - \frac{\alpha' b}{k_0}\frac{\partial}{\partial\alpha'}\left\{\frac{J_3}{\alpha'}\right\} - \frac{\beta' a}{k_0}\frac{\partial}{\partial\beta'}\left\{\frac{J_4}{\beta'}\right\}, \tag{18}$$

where

$$J_1 = \int_0^b \int_0^a \cos\alpha' k_0 u \cos\beta' k_0 v \frac{\sin k_0 r}{r}\,\mathrm{d}u\,\mathrm{d}v. \tag{19}$$

Similarly

$$J_2 = \int_0^b \int_0^a \sin\alpha' k_0 u \sin\beta' k_0 v \frac{\sin k_0 r}{r}\,\mathrm{d}u\,\mathrm{d}v,$$

$$J_3 = \int_0^b \int_0^a \sin\alpha' k_0 u \cos\beta' k_0 v \frac{\sin k_0 r}{r}\,\mathrm{d}u\,\mathrm{d}v$$

and

$$J_4 = \int_0^b \int_0^a \cos\alpha' k_0 u \sin\beta' k_0 v \frac{\sin k_0 r}{r}\,\mathrm{d}u\,\mathrm{d}v. \tag{20}$$

Rewriting u and v in polar co-ordinates; $u = r\cos\theta$ and $v = r\sin\theta$; gives J_1 as

$$4J_1 = \int\int [\sin k_0 r\ell(\theta) + \sin k_0 r\ell(-\theta) + \sin k_0 r\ell(\pi-\theta) + \sin k_0 r\ell(\pi+\theta)]\,\mathrm{d}r\,\mathrm{d}\theta, \tag{21}$$

where $\ell(\theta) = 1 - \alpha'\cos\theta - \beta'\sin\theta$.

The limits of integration in Eq. (21) must be expressed for r and θ thus

$$\int_0^b \int_0^a \frac{1}{r}\,\mathrm{d}u\,\mathrm{d}v = \left\{ \int_0^{\theta_0} \int_0^{a\sec\theta} + \int_{\theta_0}^{\pi/2} \int_0^{b\,\mathrm{cosec}\,\theta} \right\} \mathrm{d}r\,\mathrm{d}\theta, \ \text{where}\ \theta_0 = \tan^{-1}\frac{b}{a}. \tag{22}$$

The r integration is elementary and the translation of $\ell(-\theta)$, $\ell(\pi-\theta)$ and $\ell(\pi+\theta)$ onto $\ell(\theta)$ gives integrals in terms of θ in the different ranges $C_1, C_2, \ldots, C_8$ as shown in Fig. 1.

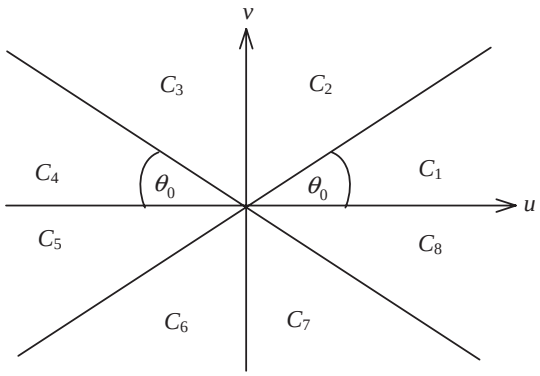

Fig. 1. The θ-integration intervals. $\theta_0 = \tan^{-1}\frac{b}{a}$.

A similar approach can be used for J_2, J_3 and J_4. Considering the interval C_1, the appropriate integrand, G_1', is found from

$$2\pi G_1' = \ell^{-1} - \frac{1-\cos(k_0 a\ell \sec\theta)}{k_0^2 ab\alpha'\beta'}\{2\ell^{-3}\alpha'\beta'\sin\theta\cos\theta - \ell^{-2}(\alpha'\cos\theta + \beta'\sin\theta) + \ell^{-1}\}$$
$$+ \frac{\sin(k_0 a\ell \sec\theta)}{k_0 ab\alpha'}\{a\alpha'\ell^{-2}\sin\theta - b\alpha'\ell^{-2}\cos\theta + b\ell^{-1} - a\ell^{-1}\tan\theta\}. \quad (23)$$

It is also found that the integrand in the interval C_5 is the same as Eq. (23) i.e., $G_5' = G_1'$. Similar forms follow for $G_2' = G_6'$, $G_3' = G_7'$ and $G_4' = G_8'$.

2.3. Radiation into a porous medium

Adopting the same approach for sound radiation into the porous medium is complicated by the term $e^{-\kappa kr}$ in the integrals of Eq. (13). However, since this is independent of α and β, where $\alpha = k_x/k$ and $\beta = k_y/k$, the method is the same up to Eq. (21) with complications only apparent when performing the r integration. The following results may be utilized:

$$\int_0^{r_0} e^{-\kappa kr}\sin kr\ell\,dr = \frac{1}{k(\kappa^2+\ell^2)}\{\ell - e^{-\kappa kr_0}[\kappa\sin kr_0\ell + \ell\cos kr_0\ell]\}, \quad (24)$$

and

$$\int_0^{r_0} e^{-\kappa kr}\cos kr\ell\,dr = \frac{1}{k(\kappa^2+\ell^2)}\{\kappa + e^{-\kappa kr_0}[\ell\sin kr_0\ell - \kappa\cos kr_0\ell]\}. \quad (25)$$

To avoid confusion, consideration is given to the first integral in expression (13) with an equivalent result following for the second integral. Considering the integrand in the interval C_1, the result equivalent to G_1' from Leppington et al. [2] is

$$4kG_1 = H_{11} + e^{-\kappa ka\sec\theta}[\sin(ka\ell\sec\theta)H_{12} + \cos(ka\ell\sec\theta)H_{13}], \quad (26)$$

where

$$H_{11} = \frac{\ell}{\kappa^2+\ell^2} - \frac{1}{k^2 ab\alpha\beta}\left\{\frac{2\alpha\beta\ell\sin\theta\cos\theta}{(\kappa^2+\ell^2)^2}\left[\frac{4\ell^2}{\kappa^2+\ell^2}-3\right] + \frac{(\alpha\cos\theta+\beta\sin\theta)}{\kappa^2+\ell^2}\left[1-\frac{2\ell^2}{\kappa^2+\ell^2}\right] + \frac{\ell}{\kappa^2+\ell^2}\right\} - \frac{\kappa}{kab\alpha\beta}\left\{\frac{2\alpha\beta\ell}{(\kappa^2+\ell^2)^2}(a\sin\theta+b\cos\theta) - \frac{(a\alpha+b\beta)}{\kappa^2+\ell^2}\right\}, \tag{27}$$

$$H_{12} = \frac{1}{kab\alpha}\left\{\frac{\alpha}{\kappa^2+\ell^2}(a\sin\theta-b\cos\theta)\left[\frac{2\ell^2}{\kappa^2+\ell^2}-1\right] + \frac{\ell}{\kappa^2+\ell^2}(b-a\tan\theta)\right\} - \frac{\kappa}{k^2 ab\alpha\beta}\left\{\frac{-1}{\kappa^2+\ell^2} + \frac{2\ell}{(\kappa^2+\ell^2)^2}(\alpha\cos\theta+\beta\sin\theta) + \frac{2\alpha\beta\sin\theta\cos\theta}{(\kappa^2+\ell^2)^2}\left[1-\frac{4\ell^2}{\kappa^2+\ell^2}\right]\right\} \tag{28}$$

and

$$H_{13} = \frac{1}{k^2 ab\alpha\beta}\left\{\frac{\ell}{\kappa^2+\ell^2} + \frac{2\alpha\beta\ell\sin\theta\cos\theta}{(\kappa^2+\ell^2)^2}\left[\frac{4\ell^2}{\kappa^2+\ell^2}-3\right] + \frac{(\alpha\cos\theta+\beta\sin\theta)}{\kappa^2+\ell^2}\left[1-\frac{2\ell^2}{\kappa^2+\ell^2}\right]\right\} - \frac{\kappa}{kab\alpha}\left\{\frac{2\alpha\ell}{(\kappa^2+\ell^2)^2}(a\sin\theta-b\cos\theta) + \frac{1}{\kappa^2+\ell^2}(b-a\tan\theta)\right\}. \tag{29}$$

Note that by setting $\kappa = 0$, the above set of equations reduces to

$$4kG_1 = H_{11} + \sin(ka\ell\sec\theta)H_{12} + \cos(ka\ell\sec\theta)H_{13}, \tag{30}$$

where

$$H_{11} = \ell^{-1} - \frac{1}{k^2 ab\alpha\beta}\{2\ell^{-3}\alpha\beta\sin\theta\cos\theta - \ell^{-2}(\alpha\cos\theta+\beta\sin\theta) + \ell^{-1}\}, \tag{31}$$

$$H_{12} = \frac{1}{kab\alpha}\{a\alpha\ell^{-2}\sin\theta - b\alpha\ell^{-2}\cos\theta + b\ell^{-1} - a\ell^{-1}\tan\theta\} \tag{32}$$

and

$$H_{13} = \frac{1}{k^2 ab\alpha\beta}\{2\ell^{-3}\alpha\beta\sin\theta\cos\theta - \ell^{-2}(\alpha\cos\theta+\beta\sin\theta) + \ell^{-1}\}, \tag{33}$$

which are the same as Leppington et al. [2] (Eq. (23)) since $k = k_0$.

In the interval C_5 it is discovered that G_5 can be found by substituting $-\kappa$ for κ in G_1. Similar expressions are also found in the other regions.

Terms like ℓ^{-1} appearing in the problem considered by Leppington et al. [2] appear here as $\ell(\kappa^2+\ell^2)^{-1}$. Since much of their analysis considered regions where $\ell^{-1}\to\infty$, the same approach is not necessary here because $\ell(\kappa^2+\ell^2)^{-1}$ is always finite for $\kappa > 0$. In fact, $\kappa\to 1$ from below as $f\to 0$ and $\kappa\to 0$ from above as $f\to\infty$ (see Refs. [5,6]) but in the above coincidence solution of Leppington et al. [2], $\ell(\theta)$ has no zeros. In the following it transpires that this is unimportant because coincidence is not a consideration for finding a leading order solution.

It is now important to investigate the behaviour of the exponential appearing in Eq. (26) and the equivalent terms for $G_2, \ldots, G_8$. Now $\kappa > 0$ so letting $N = \kappa ka$ and $M = \kappa kb$ such that M and

N are both positive, the terms appear as $e^{-N\sec\theta}$ in C_1 and C_8, $e^{N\sec\theta}$ in C_4 and C_5, $e^{-M\,\mathrm{cosec}\,\theta}$ in C_2 and C_3 and $e^{M\,\mathrm{cosec}\,\theta}$ in C_6 and C_7. However, $\sec\theta > 1$ in C_1 and C_8 and $\sec\theta < -1$ in C_4 and C_5. Thus, it always occurs in the form $e^{-N'}$ where $N' > 0$. A similar argument in the other regions gives rise to the form $e^{-M'}$ where $M' > 0$.

To simplify the problem, the asymptotic limit as $k\kappa\hat{a} \to \infty$ (where $\hat{a}$ is the lesser of a and b) is considered. Since $\kappa < 1$, then $k\hat{a} > k\kappa\hat{a}$ so $k\hat{a} \to \infty$ also. This implies that the acoustic wavelengths in the system are much smaller than the plate dimensions.

Therefore, in the limit as $k\kappa\hat{a} \to \infty$, $N' \to \infty$ and $M' \to \infty$ and $e^{-N'} \to 0$ and $e^{-M'} \to 0$, so in each of the intervals C_i

$$4kG_i \sim H_{i1}, \tag{34}$$

to leading order where $i = 1, 2, \ldots, 8$. Furthermore,

$$H_{i1} = \frac{\ell}{\kappa^2 + \ell^2} + O\left(\frac{1}{k\hat{a}}\right), \tag{35}$$

so

$$4kG_i \sim \frac{\ell}{\kappa^2 + \ell^2}. \tag{36}$$

This, along with the corresponding term for the second integral in Eq. (13), gives

$$\sigma \sim \frac{\rho c}{\rho_0 c_0} \frac{1}{2\pi} \int_0^{2\pi} \left\{ \frac{\ell + \tau\kappa}{\kappa^2 + \ell^2} \right\} \mathrm{d}\theta. \tag{37}$$

This integral can be evaluated to give

$$\sigma \sim \frac{\rho c}{\rho_0 c_0} \frac{1}{\sqrt{2(\lambda^2 + 4\kappa^2)}} \{[(\lambda^2 + 4\kappa^2)^{1/2} + \lambda]^{1/2} + \tau[(\lambda^2 + 4\kappa^2)^{1/2} - \lambda]^{1/2}\}, \tag{38}$$

where $\lambda = 1 - \kappa^2 - \mu^2$ and $\mu^2 = \alpha^2 + \beta^2 = (k_p/k)^2$.

This is the leading order solution, which is area dependent and applies over the whole frequency spectrum (assuming f is large enough to allow $k\kappa\hat{a} \gg 1$). Therefore the plate behaves as if it is infinite and the edge terms (which dominate below coincidence for radiation into air) can be neglected. The following section considers the simpler problem of radiation from an infinite plate and shows that the same result, Eq. (38), is obtained.

3. Radiation from an infinite plate

3.1. Radiation from an infinite plate into air

Leppington et al. [2] showed that sound radiation into *air* depends crucially on the relative magnitudes of the acoustic wavenumber, k_0, and the plate wavenumber $k_p = (k_x^2 + k_y^2)^{1/2}$. Coincidence occurs when the trace acoustic wavenumber equals the plate wavenumber and the critical coincidence frequency occurs at the lowest frequency at which they are equal. The effect on radiation can be illustrated by considering an infinite plate excited in such a way as to vibrate with transverse velocity $U(x, y) = U_0 \sin k_x x \sin k_y y \exp(\mathrm{i}\omega t)$. The motion of the air can be described by

a velocity potential ϕ_0 which satisfies the wave equation:

$$\nabla^2\phi_0 = \frac{1}{c_0^2}\frac{\partial^2\phi_0}{\partial t^2} \tag{39}$$

(where $c_0 = \omega/k_0$ is the wavespeed in air) and the boundary condition

$$\frac{\partial\phi_0}{\partial z} = U(x,y) \text{ on } z = 0. \tag{40}$$

The solution is

$$\phi_0 = \frac{U_0}{\mathrm{i}\gamma_0}\sin k_x x \sin k_y y \exp \mathrm{i}(-\gamma_0 z + \omega t), \tag{41}$$

where $\gamma_0^2 = k_0^2 - k_x^2 - k_y^2$ i.e., $\gamma_0 = 0$ at the critical coincidence frequency. If $k_0 > (k_x^2 + k_y^2)^{1/2}$ then γ_0 is real and this is known as 'above' coincidence. Conversely, if $k_0 < (k_x^2 + k_y^2)^{1/2}$, then γ_0 is imaginary and this is referred to as 'below' coincidence. It is useful to define γ_0 thus,

$$\gamma_0 = (k_0^2 - k_x^2 - k_y^2)^{1/2} \text{ for } k_0 > (k_x^2 + k_y^2)^{1/2} \tag{42}$$

and

$$\gamma_0 = -\mathrm{i}(k_x^2 + k_y^2 - k_0^2)^{1/2} = -\mathrm{i}\gamma_0', \text{ say, for } k_0 < (k_x^2 + k_y^2)^{1/2},$$

where γ_0' is real.

The waves are described by the real part of ϕ_0. Above coincidence

$$\mathrm{Re}\{\phi_0\} = -\frac{U_0}{\gamma_0}\sin k_x x \sin k_y y \sin(\gamma_0 z - \omega t), \tag{43}$$

which represents a radiating sound field away from the plate. Below coincidence

$$\mathrm{Re}\{\phi_0\} = \frac{U_0}{\gamma_0'}\sin k_x x \sin k_y y \, \mathrm{e}^{-\gamma_0' z}\cos \omega t, \tag{44}$$

which represents exponentially decaying surface waves as $z \to \infty$.

These two results are reflected in the radiation efficiency σ_0 defined by

$$\sigma_0 = \frac{W_0}{\rho_0 c_0 \langle U^2 \rangle} = \frac{W_0}{\frac{1}{8}\rho_0 c_0 U_0^2}, \tag{45}$$

where $W_0 = -\frac{1}{2}U_0^2\rho_0\omega \,\mathrm{Im}\{\int\int \phi_0(x,y,0)\phi_{0z}^*(x,y,0)\,\mathrm{d}x\,\mathrm{d}y\}$ is the time-averaged power. The integration is performed to give power per unit area of plate. The term $\phi_0\phi_{0z}^*$ is imaginary above coincidence (due to γ_0 being real) giving a radiation efficiency

$$\sigma_0 = k_0/\gamma_0. \tag{46}$$

Below coincidence $\phi_0\phi_{0z}^*$ is purely real so

$$\sigma_0 = 0, \tag{47}$$

and no power is radiated.

The physical explanation for this is described by the cancelling phenomenon known as hydrodynamic short circuiting. Below coincidence sound in air travels faster than the bending waves on the plate and therefore disturbances in the air caused by plate vibrations result in the air

moving sideways thus cancelling the pressure differences and resulting in no net radiation away from the plate.

In finite sized plates there is no cancellation of the acoustic pressure around the edges and so radiation can occur below coincidence, the strength of which is proportional to the perimeter length of the plate. The approximate equation given by Leppington et al. [2] for radiation in this case is then

$$\sigma = \frac{\sum L c_0}{4\pi^2 f^{1/2} f_c^{1/2} S(\mu^2-1)^{1/2}}\left[\ln\left(\frac{\mu+1}{\mu-1}\right)+\frac{2\mu}{\mu^2-1}\right], \tag{48}$$

where $\sum L$ is the perimeter length, S is the surface area, f_c is the critical coincidence frequency and $\mu = (f_c/f)^{1/2}$.

3.2. Radiation from an infinite plate into a porous medium

For the same infinite plate radiating into a porous medium with acoustic wave number k_a, the fluid motion within the porous medium is given by

$$\phi_a = \frac{U_0}{\mathrm{i}\gamma_a}\sin k_x x \sin k_y y \exp \mathrm{i}(-\gamma_a z + \omega t). \tag{49}$$

Here $\gamma_a = (k_a^2 - k_x^2 - k_y^2)^{1/2}$ but k_a can be expressed as $k(1-\mathrm{i}\kappa)$ as before. Thus γ_a can be written as

$$\gamma_a = g^{1/2}(\cos\tfrac{1}{2}\varphi + \mathrm{i}\sin\tfrac{1}{2}\varphi) \tag{50}$$

where $g = \{[k^2(1-\kappa^2) - k_x^2 - k_y^2]^2 + 4k^4\kappa^2\}^{1/2}$ and $\varphi = \tan^{-1}\left\{\frac{-2k^2\kappa}{k^2(1-\kappa^2)-k_x^2-k_y^2}\right\}$, $-\pi<\varphi<\pi$. In fact, since γ_a is required to be single-valued, φ must be chosen such that $-\pi<\varphi<0$. Substitution for k_x and k_y in terms of their non-dimensional counterparts α and β gives $g = k^2(\lambda^2+4\kappa^2)^{1/2}$ and $\varphi = \tan^{-1}(-2\kappa/\lambda)$.

It was shown for air that $\sigma_0 = 0$ when γ_0 is purely imaginary. In the porous medium γ_a is only purely imaginary when $\varphi = \pm(2n+1)\pi$, all of which are outside the range of definition. So it is anticipated that the whole area of the plate will radiate sound both above and below coincidence. The waveforms in the fluid are given by

$$\mathrm{Re}\{\phi_a\} = \frac{1}{g^{1/2}}\sin k_x x \sin k_y y \exp(-g^{1/2}\sin\tfrac{1}{2}\varphi z)\sin(g^{1/2}\cos\tfrac{1}{2}\varphi z - \tfrac{1}{2}\varphi - \omega t). \tag{51}$$

This expression contains both the radiating sine term associated with Eq. (43) and a decaying exponential as in Eq. (44). There is therefore a radiating sound field, which decays with distance due to the dissipative nature of the medium.

The radiation efficiency is given by

$$\sigma_a = \frac{W_a}{\frac{1}{8}\rho_0 c_0 U_0^2}, \tag{52}$$

where

$$W_a = -\tfrac{1}{2}U_0^2\omega\,\mathrm{Im}\{\rho_a\int\int \phi_a(x,y,0,t)\phi_{az}^*(x,y,0,t)\,\mathrm{d}x\,\mathrm{d}y\}. \tag{53}$$

The solution is

$$\sigma_a = \frac{\rho k_0}{\rho_0 g^{1/2}} (\cos \tfrac{1}{2}\varphi - \tau \sin \tfrac{1}{2}\varphi) \tag{54}$$

which can also be expressed as

$$\sigma_a = \frac{\rho c}{\rho_0 c_0} \frac{1}{\sqrt{2(\lambda^2 + 4\kappa^2)}} \{[(\lambda^2 + 4\kappa^2)^{1/2} + \lambda]^{1/2} + \tau[(\lambda^2 + 4\kappa^2)^{1/2} - \lambda]^{1/2}\}. \tag{55}$$

The right-hand side of this expression is identical to that of Eq. (38) and so it is apparent that

$$\sigma \sim \sigma_a. \tag{56}$$

Therefore the leading order approximation for radiation efficiency of a finite plate radiating into a porous medium is the same as the radiation efficiency of an infinite plate.

At high frequencies, for materials with tortuosity and porosity close to 1, the values of τ and κ will tend to zero and ρc will tend to $\rho_0 c_0$. Therefore, where $f > f_c$, Eq. (55) simplifies to $\sigma = 1/\sqrt{\lambda} = (1 - f_c/f)^{-1/2}$, which is the standard equation for radiation into air above the critical frequency.

4. Experimental results

In order to test the theory that was developed in the previous sections, measurements were made on two thin plates radiating into a porous layer of finite thickness. As it is difficult to make a direct measurement of the sound field generated in the porous layer, partly due to the difficulties of placing a microphone in the porous layer and partly because the acoustic energy radiated is converted into heat within a short distance from the plate, the approach adopted was to measure the damping loss of the plate. The plate was excited with a blow from a small hammer and the reverberation time, T, was measured using an accelerometer (at 6 positions) from which the damping loss factor, η, was found using the equation

$$\eta = \frac{2.2}{fT}. \tag{57}$$

The predicted damping loss factor due to radiation was found from the equation

$$\eta = \frac{\rho_0 c_0 \sigma_a}{\omega \rho_s}, \tag{58}$$

where ρ_s is the plate surface density. (Note that $\rho_0 c_0$ is used as σ_a was normalised by $\rho_0 c_0$ in Eq. (52).)

To calculate the properties of the equivalent fluid the Allard and Champoux [5] expressions were used. For fibrous materials, they give ρ_a and c_a as

$$\rho_a = 1.2 + \left(\frac{-0.0364}{(\rho_0 f/R)^2} - \frac{\mathrm{i}0.1144}{(\rho_0 f/R)} \right)^{1/2} \tag{59}$$

and

$$c_a = \left(\frac{101320}{\rho_a} \times \frac{\mathrm{i}29.64 + (2.82/(\rho_0 f/R)^2 + \mathrm{i}24.9/(\rho_0 f/R))^{1/2}}{\mathrm{i}21.17 + (2.82/(\rho_0 f/R)^2 + \mathrm{i}24.9/(\rho_0 f/R))^{1/2}} \right)^{1/2}, \tag{60}$$

where R is the air flow resistivity Rayls/m. These expressions can then be used to give $\tau = -\mathrm{Im}(\rho_a)/\mathrm{Re}(\rho_a)$ and $\kappa = -\mathrm{Im}(k_a)/\mathrm{Re}(k_a)$. The value of μ is found from

$$\mu^2 = \frac{k_p^2}{k^2} = \frac{4\pi^2 f f_c}{c_0^2 (\mathrm{Re}(k_a))^2}. \tag{61}$$

These values can then be inserted into Eq. (38) to give the radiation efficiency. Equivalent fluid properties may also be found using the expressions given in Refs. [6–9].

The predicted loss factor was determined by summing the measured damping of a freely suspended plate, taken to be the internal loss factor, and the predicted radiation into a porous layer.

The tests were made on thin aluminium plates radiating into a 200 and a 50 mm thick semi-rigid rockwool slab with a flow resistivity of 40,000 Rayls/m. Measurements were made with the plate resting directly on the layer and also when supported on 5 mm spacers. The porous layer rested on a concrete floor. The thickness of the gap could not be set accurately as the spacers tended to sink into the porous layer and because of bending of the plate (due to self-weight) and probably varied from 1–5 mm. The presence of the air gap will tend to reduce the radiation from the plate and so reduce the measured damping [1]. However, fibrous wisps of porous material were still lightly in contact with the plate and this will increase the measured damping so the two effects will tend to cancel out.

The two sets of measurements allow the effect of damping, caused by contact between the plate and the porous layer, to be estimated as there will be no structural damping if there is an air gap.

The first test was performed on a 0.95×0.85 m $\times$ 1.5 mm aluminium plate and the results are shown in Fig. 2. The second test was performed on a 0.7×0.5 m $\times$ 0.67 mm aluminium plate radiating into the same porous layer and the results can be seen in Fig. 3.

In each case the dotted line shows the damping of the plate when suspended by thin strings and gives damping much less than when the plate is close to or touching the porous layer. Placing the plate over the layer but not quite touching it increases the damping and the measured data agree well with the predicted curve. There is little difference between the results for a 200 and 50 mm layer suggesting that for this porous material the theory (which is based on an infinitely thick layer) works well even when the layer is far from infinite in thickness. This might be expected for the thicker layer as the attenuation through the layer and back from the concrete would be at least 10 dB from 27 Hz but for the 50 mm layer the attenuation is only 10 dB from 450 Hz. In Fig. 2 the radiation into the thin layer gives a slightly higher damping whereas in Fig. 3 the damping is a little lower. Given the difficulties in setting the spacing and in the experimental uncertainties, this difference cannot be taken as significant. At low frequencies the measured results are less than predicted. This may be because the requirement that the plate be large compared to a wavelength ($k\kappa\hat{a}$ is large) is not satisfied though $k\kappa\hat{a}$ is already 12 at 200 Hz. Alternatively it may be due to the air gap which allows waves to travel laterally when the impedance of the layer is high (as at low frequencies).

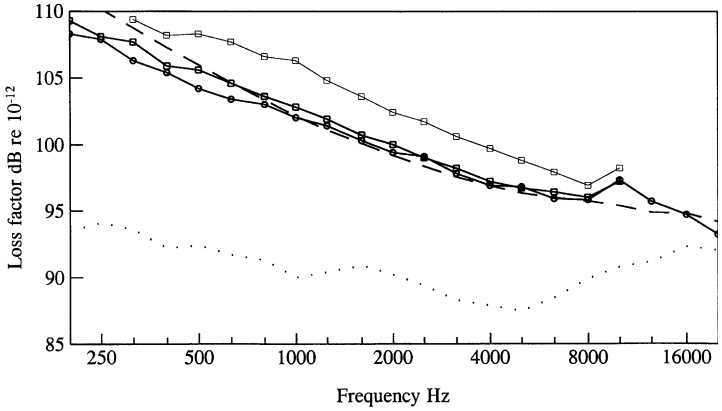

Fig. 2. Measured and predicted damping loss factor of a 1.5 mm thick aluminium plate when radiating into a porous layer. ——, measured when resting on the porous layer; ——, measured when placed above the porous layer; . . . . . , measured damping of a freely suspended plate; - - - - -, predicted damping when radiating into a porous layer; ○, 200 mm porous layer; □, 50 mm porous layer.

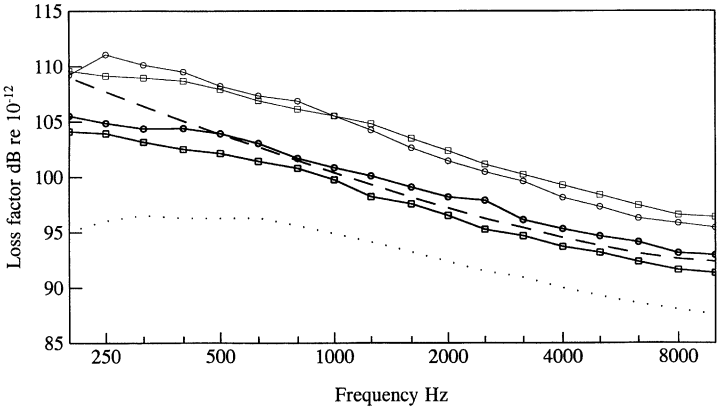

Fig. 3. Measured and predicted damping loss factor of a 0.67 mm aluminium plate when radiating into a porous layer. ——, measured when resting on the porous layer; ——, measured when placed above the porous layer; . . . . . , measured damping of a freely suspended plate; - - - - -, predicted damping when radiating into a porous layer; ○, 200 mm porous layer; □, 50 mm porous layer.

When the plate is resting on the porous layer then the damping of the thicker plate (Fig. 2) increases by about 3 dB and the thinner plate (Fig. 3) increases by about 5 dB. This increase will be in part due to the increased radiation but is probably due mainly to the structural damping. An increase of 3 dB would mean that the radiation damping and structural damping were equal.

5. Discussion

The use of an equivalent fluid representation of the porous material gives an equation for sound radiation from a finite plate that is tractable using analytical techniques. The resulting solution

provides a relatively simple method for predicting radiation at high frequency, where the plate exhibits multimodal behaviour. There are, however, a number of assumptions in the theory that limit its application.

The first is related to the adoption of an equivalent fluid representation of the porous material where contact between the fluid and the plate is implicit but where it is assumed that no contact occurs between the skeleton and the plate. This does not therefore account for the viscoelastic behaviour of the structural phase of the porous medium, which if in contact with the plate will support longitudinal and shear waves. As a result, the damping for a real system, where there is physical contact, might reasonably be expected to be higher than predicted by the theory presented in this paper as was observed in the experimental data. The degree to which this additional radiation mechanism affects the behaviour of a plate is, however, dependent on the viscoelastic properties of the structural phase of the porous medium. For very limp materials, such as glass wool, evidence suggests that the influence of the structural phase is secondary to that of the fluid phase [10]. It is therefore likely that the expression for radiation should be reliable even if used for systems where there is contact between the plate and the porous medium. It might reasonably be expected that where the porous material is not bonded directly to the plate and where there is not continuous contact between the two that the effect of the structure would be reduced further. In many practical applications, contact may be incomplete or there may be the deliberate introduction of a small air gap. The presence of an air gap will influence radiation but previous work has indicated that reasonably accurate predictions of radiation can be obtained for systems where the gap is narrow [1]. Care has to be exercised for systems where the porous layer has a high flow resistivity as this can result in the acoustic disturbance travelling laterally along the air space in preference to penetrating the porous medium.

There have also been numerical studies carried out using the Biot representation [10] of the porous medium which accounts for both the fluid and the structural phases. It is probable, however, that these will still be subject to limitations when the nature of the interface between the plate and the porous medium is indeterminate. If a more detailed solution for radiation into a porous medium is required then a more complete model of the porous layer could be used. This would not be practical with the full solution for radiation from a finite plate but as the leading order terms can be found from consideration of an infinite plate then this simpler model could be used as a basis for further calculations of radiation in this case.

Predictions at low frequency are affected both by the assumption of multi modal behaviour and by the assumption that $k\kappa\hat{a} \gg 1$ in performing the asymptotic solution. The number of modes present in the plate may be predicted accurately from a knowledge of the plate material and its physical properties. Similarly, $k\kappa\hat{a}$ may readily be evaluated from the plate properties and an equivalent fluid representation of the porous material. An example of the probable effect that this may have on the prediction may be seen in Fig. 3 in a related paper where the theory is compared with numerical solutions of Eq. (13) [11]. At low frequencies the evaluation of the leading order term in the current theory yields a solution equivalent to the infinite plate solution and so omits edge and corner effects resulting from incomplete phase cancellation at the boundaries of a finite plate. The evaluation of the higher order terms in Eqs. (31)–(33) (as well as the equivalent terms for the second integral in Eq. (13)) would yield expressions for these effects.

The final restriction relates to the treatment of the porous medium as being of semi infinite extent, which implies that there will be no reflected field incident on the plate. In practice, for

layers of finite thickness, this will not be the case and reflections occurring at the boundaries of the porous layer will give rise to a reflected wavefield incident on the plate. Most porous materials offer very high attenuation with distance and as a result, for all but very thin layers, the magnitude of any reflected field is likely to be insignificant. A rough estimate of the strength of the returning field could be made using the equivalent fluid representation of the propagation coefficient and an assumed value for the reflection coefficient for the free face of the porous layer.

When an infinite plate is radiating into air below the critical frequency, there are no waves radiating away from the plate and the air molecules move in an elliptical path with an amplitude that decreases with distance. As the medium is not dissipative there is no energy lost from the plate. When an infinite plate is radiating into a porous medium, there are both travelling plane waves and the elliptical motion associated with nearfield waves. As the medium is itself dissipative there is energy lost as the molecules move in elliptical paths in addition to the energy lost as travelling waves (which are themselves attenuated with distance) resulting both in higher values for radiation and expressions for radiation which are dependant on the area of the plate.

The general trend in the radiation efficiency curves can be seen in Figs. 4 and 5. Fig. 4 shows how the radiation efficiency of a plate with a critical frequency of 16,000 Hz (when radiating into air) varies as the air flow resistivity of the porous layer varies from 100 to 100,000 Rayls/m. It can be seen that as the air flow resistivity tends to zero, the peak in the radiation efficiency at the critical frequency becomes sharper and below the critical frequency, the radiation efficiency tends to zero. In such cases the radiation efficiency of a real plate will be dominated by edge effects which are not included in this figure. However, a practical solution would be to add the radiation due to edge effects for radiation into air (Eq. (48)) to the radiation into the porous layer over the surface to give an estimate of the total radiation.

Fig. 5 shows how the radiation efficiency of a plate radiating into a porous medium with an air flow resistivity of 10,000 Rayls/m changes as the critical frequency varies from 100 to 20,000 Hz. The critical frequency is indicated by a small vertical tick in the curve. It can be seen that when the critical frequency is low the peak is smoothed out and the radiation efficiency is relatively insensitive to the actual value of f_c.

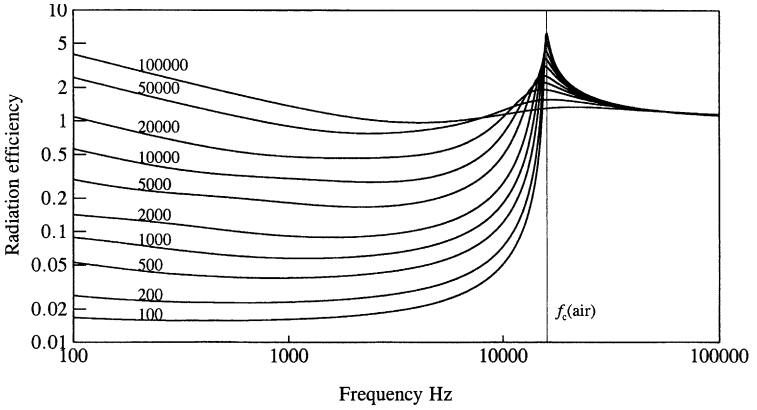

Fig. 4. Radiation efficiency of a plate radiating into a porous medium with air flow resistivity of 100–100,000 Rayls/m.

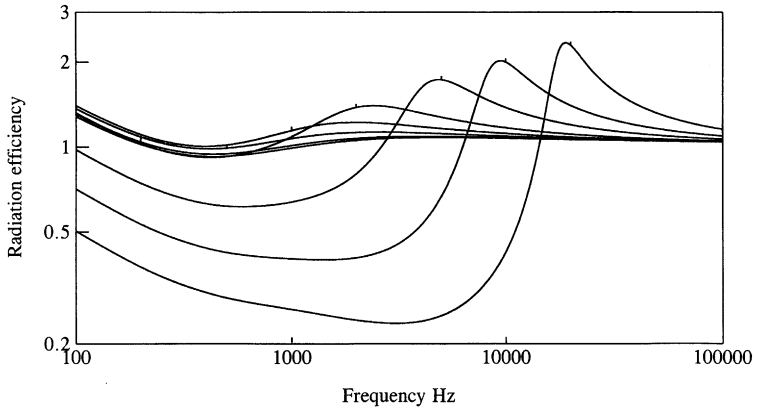

Fig. 5. Radiation efficiency of a plate radiating into a porous medium with air flow resistivity of 100,000 Rayls/m as the critical frequency (in air) changes from 100 to 20,000 Hz.

6. Conclusions

The results of this work have shown that when a plate radiates into a porous layer, the radiation will be much higher than for radiation into air. Radiation takes place over the entire plate. A knowledge of this allows a simpler infinite plate theory to be used to calculate the radiation efficiency. The ability to use the infinite plate theory to calculate radiation will allow other more complex problems to be solved such as radiation into layers of finite thickness, radiation into multiple layers (including air gaps) and radiation into porous layers whose structure is such that they cannot be modelled as equivalent fluids.

Acknowledgements

This work was funded by the Engineering and Physical Sciences Research Council (EPSRC) and the Defence Evaluation Research Agency (DERA) on a grant held jointly by Heriot-Watt University, the University of Hull and the University of Nottingham.

References

[1] A. Cummings, H.J. Rice, R. Wilson, Radiation damping in plates induced by porous media, *Journal of Sound and Vibration* 221 (1999) 143–167.

[2] F.G. Leppington, E.G. Broadbent, K.H. Heron, The acoustic radiation efficiency of rectangular panels, *Proceedings of the Royal Society of London A* 382 (1982) 245–271.

[3] G. Maidanik, Response of ribbed panels to reverberant acoustic fields, *Journal of the Acoustical Society of America* 34 (1962) 809–826.

[4] C.E. Wallace, Radiation resistance of a rectangular plate, *Journal of the Acoustical Society of America* 51 (1972) 946–952.

[5] J.-F. Allard, Y. Champoux, New empirical equations for sound propagation in rigid frame fibrous materials, *Journal of the Acoustical Society of America* 91 (6) (1992) 3346–3353.

[6] F.P. Mechel, Design charts for sound absorber layers, *Journal of the Acoustical Society of America* 83 (3) (1988) 1002–1013.
[7] M.E. Delany, E.N. Bazley, Acoustical properties of fibrous absorbent materials, *Applied Acoustics* 3 (1970) 105–116.
[8] R. Kirby, A. Cummings, Prediction of the bulk acoustic properties of fibrous materials at low frequencies, *Applied Acoustics* 56 (1999) 101–125.
[9] A. Cummings, P. Beadle, Acoustic properties of reticulated plastic foams, *Journal of Sound and Vibration* 175 (1993) 115–133.
[10] R. Panneton, N. Atalla, Numerical prediction of sound transmission through finite multiplayer systems with poroelastic materials, *Journal of the Acoustical Society of America* 100 (1) (1996) 346–354.
[11] A. Cummings, Sound radiation from a plate into a porous medium, *Journal of Sound and Vibration* 247 (3) (2001) 389–406.